Dyes and Pigments 92 (2012) 1114–1121

Contents lists available at ScienceDirect

Dyes and Pigments

journal homepage: www.elsevier.com/locate/dyepig

Synthesis and spectroelectrochemistry of new phthalocyanines with ester functionalities

Altuğ Mert Sevim [a], Sibel Arıkan [a], Atıf Koca [b], Ahmet Gül [a,*]

[a] Department of Chemistry, Istanbul Technical University, 34469 Maslak, Istanbul, Turkey
[b] Department of Chemical Engineering, Faculty of Engineering, Marmara University, 34722 Göztepe, Istanbul, Turkey

ARTICLE INFO

Article history:
Received 30 May 2011
Received in revised form
21 June 2011
Accepted 22 July 2011
Available online 4 August 2011

Dedicated to Professor Michael Hanack on the occasion of his 80th birthday.

Keywords:
Phthalocyanine
Esterification
Electrochemistry
Spectroelectrochemistry
Electrocolorimetry
DCC

ABSTRACT

Metal-free (H_2Pc) and metallophthalocyanines (MPc; M: Co, Zn) with four *n*-pentyl ester of thioglycolic acid groups have been synthesized by the esterification of the corresponding carboxylic acid derivatives with *n*-pentanol. The novel phthalocyanine compounds were characterized by elemental analyses, mass, FT-IR and UV–Vis spectral data. The aggregation investigations carried out in different concentrations and solvents indicate that ester substituted metal-free and metallo-phthalocyanine compounds have not shown any aggregation behavior in the concentration range of about 10^{-5} M. Electrochemical and in-situ spectroelectrochemical measurements give common MPc based redox behaviors which supported the proposed structure of the complexes. While CoPc gives both metal-based and ring-based redox processes, H_2Pc and ZnPc give only ring-based electron transfer processes. In-situ electrocolorimetric method was applied to investigate the color of the electro-generated anionic and cationic forms of the complexes.

1. Introduction

Phthalocyanines (Pc) are two-dimensional 18 π-electron aromatic porphyrin (Por) synthetic analogs consisting of four isoindole units linked together through nitrogen atoms. Phthalocyanines and their metallo derivatives (MPcs) have recently attracted an increasing interest not only for the preparation of dyes and pigments but also as building blocks for the construction of new molecular materials for electronics and optoelectronics. Numerous properties arise from their electronic delocalization, which makes them valuable in different fields of science and technology such as photoconducting agents in photocopying devices, chemical sensors, electrocatalyst, data storage systems, liquid crystals and photosensitizer in photodynamic therapy [1–3].

All the applications of phthalocyanines are related to their high chemical and thermal stability, which, in turn, is closely related to their electrochemical properties. It is well-known that the electrochemical and spectroscopic properties of phthalocyanine derivatives can be tuned by either varying the central metal atom or alternating the type, number, and positions of the substituents on the macrocycle ligands [4]. Solubility is a key feature for phthalocyanines and most of their behaviors are best investigated in soluble form. A common means for preparing soluble phthalocyanines is to attach functional groups like tertiary butyl or hexyl groups, amide groups, carboxylic acid and sulfonic acid groups [5–10], bulky groups such as crown ether [11–13], azo groups [14], etc. at the peripheral and axial positions of phthalocyanine ring. Compared to unsubstituted parent metal phthalocyanines, ester-containing porphyrazines and phthalocyanines are highly soluble in chlorinated hydrocarbons [15].

The phthalocyanine unit with an 18π electron aromatic system and the metal center in some cases are capable of oxidation and reduction. These redox processes depend on various factors such as the type of the central metal atoms, axial ligands, substituents and solvent. The redox properties of phthalocyanines are critically related to most of their industrial applications. MPcs containing redox active transition metal ions such as Co^{2+} and Mn^{3+} are known to be very effective electrochemical sensors and electrocatalysts under heterogeneous and homogenous conditions [1,2].

Recently, we have reported on the synthesis and characterization of carboxylic acid substituted metal-free and metallophthalocyanines (Zn, Co) [10]. In this paper all of the thioglycolic acid substituents of the metal-free and metallophthalocyanines were esterified with

* Corresponding author. Tel.: +90 212 285 68 27; fax: +90 212 285 63 86.
E-mail address: ahmetg@itu.edu.tr (A. Gül).

0143-7208/$ – see front matter © 2011 Elsevier Ltd. All rights reserved.
doi:10.1016/j.dyepig.2011.07.015

n-pentanol for gaining higher solubility in nonpolar solvents. Total esterification of all carboxyl groups in metal-free phthalocyanine **2** and metallophthalocyanines **2a**–**b** was accomplished in pyridine in the presence of dicyclohexylcarbodiimide (DCC) and 4-toluenesulfonic acid (p-TSA) as catalysts. We have also investigated the electrochemical and in-situ spectroelectrochemical properties of newly synthesized phthalocyanines to determine their possible applications in various electrochemical technologies.

2. Experimental

2.1. Materials and equipment

All reactions were carried out under nitrogen atmosphere in dried solvents. The solvents were stored over molecular sieves. All reagents and solvents were of reagent grade quality obtained from commercial suppliers. 4-nitrophthalonitrile was synthesized according to published methods [16]. 4-(carboxymethylsulfanyl)phthalonitrile (**1**), tetrakis(4-carboxymethylsulfanyl) phthalocyanine (**2**), tetrakis(4-carboxymethyl sulfanyl) cobalt(II) phthalocyanine (**2a**) and tetrakis(4-carboxymethylsulfanyl) zinc(II)phthalocyanine (**2b**) were prepared as reported earlier [10].

IR spectra were recorded on a Perkin–Elmer Spectrum One FT-IR (ATR sampling accessory) spectrophotometer, and electronic spectra were recorded on a Scinco Neosys-2000 double-beam ultraviolet–visible (UV–vis) spectrophotometer using 1 cm path length cuvettes at room temperature. ^{1}H NMR spectra were recorded with a Bruker 200 MHz FT-NMR spectrometer. Mass spectra were performed on Ultima Fourier Transform and Varian 711 mass spectrophotometer. Elemental analyses were performed by the Instrumental Analysis Laboratory of the TUBITAK Marmara Research Center. The homogeneity of the products was tested in each step by TLC.

2.2. 2,9,16,23-Tetrakis(pentyloxycarbonylmethylsulfanyl) phthalocyanine derivatives (**3**, **3a**–**b**)

A mixture of the phthalocyanine derivative [**2**(0.070 g), **2a**(0.090 g) or **2b**(0.095 g), 0.08 mmol], dicyclohexylcarbodiimide (DCC) (0.165 g, 0.8 mmol), *p*-toluenesulfonic acid (0.014 g, 0.08 mmol) and *n*-pentanol (0.05 ml, 0.4 mmol) was stirred in dry pyridine (15 ml) under N_2 for 48 h at 60 °C. The contents were filtered and the filtrate was evaporated to dryness. The residue was treated with CH_2Cl_2 (20 ml) and the clear solution was extracted with 50 ml of 10% Na_2CO_3 solution. The extraction was repeated for two times with water and dried with anhydrous Na_2SO_4, filtered, then evaporated to dryness again. The product was stirred with cold ethanol (20 ml) in ice bath for 6 h, filtered and then washed with acetonitrile, methanol, hexane and diethyl ether. Finally the green precipitate was purified by column chromatography.

2.2.1. 2,9,16,23-Tetrakis(pentyloxycarbonylmethylsulfanyl) phthalocyanine (**3**)

Purification of the product was accomplished by column chromatography on silica gel first with hexane/THF (2:1) and then with THF as eluent. This product is soluble in chloroform, dichloromethane, THF, DMF, DMSO. Yield 0.022 g (32%). M.p. > 250 °C. IR $\upsilon_{max}/(cm^{-1})$: 3287 (N–H), 3080 (Ar-H), 2927–2854 (alkyl CH), 1729 (C=O), 1602–1448 (Ar C=C), 1130–1107(ester C–O), 1008, 894, 819, 742. ^{1}H NMR ($CDCl_3$, δ ppm): 7.17–6.96 (br, 12H, Ar-H), 4.97 (t, 8H, OCH_2), 3.74 (s, 8H, SCH_2), 1.84–1.25 (m, 24H, CH_2), 0.86 (t, 12H, CH_3); UV–Vis λ_{max} (nm) ($\log\varepsilon$) in $CDCl_3$: 342(4.61), 675(4.63), 708 (4.58). MS (MALDI-TOF): *m*/*z* 1156.4 $[M+H]^+$Anal. Calc. for $C_{60}H_{37}N_8O_8S_4$: C, 62.31; H, 3.20; N, 9.70; Found: C, 61.92; H, 3.12; N, 9.78%.

2.2.2. 2,9,16,23-Tetrakis(pentyloxycarbonylmethylsulfanyl) phthalocyaninatocobalt (II) (**3a**)

The green product was purified by column chromatography with silica gel using firstly hexane/THF (5:1) then, THF as eluent. This dark green compound is soluble in chloroform, dichloromethane, THF, DMF, DMSO. Yield 0.028 g (24%). M.p. > 250 °C. IR $\upsilon_{max}/(cm^{-1})$: 3054 (Ar-H), 2936–2856 (alkyl CH), 1728 (C=O), 1600–1449(Ar C=C), 1137–1105(ester C–O), 1042, 931, 890, 818, 750. UV–Vis λ_{max}(nm)($\log\varepsilon$) in $CDCl_3$: 315(4.13), 680(4.08). MS (MALDI-TOF): *m*/*z* 1213.6 $[M+H]^+$. Anal. Calc. for $C_{60}H_{64}N_8O_8S_4Co$: C, 59.39; H, 5.28; N, 9.24; Found: C, 59.44; H, 5.21; N, 9.29%.

2.2.3. 2,9,16,23-Tetrakis(pentyloxycarbonylmethylsulfanyl) phthalocyaninatozinc (II) (**3b**)

The product was purified by column chromatography with silica gel using firstly hexane/THF (5:1) then, THF as eluent. This green compound is soluble in chloroform, dichloromethane, THF, DMF, DMSO. Yield 0.033 g (27%). M.p. > 250 °C. IR $\upsilon_{max}/(cm^{-1})$: 3048 (Ar-H), 2925–2855 (alkyl CH), 1726 (C=O), 1599–1451 (Ar C=C), 1134–1100(ester C–O), 1036, 976, 909, 818, 760, 741. ^{1}H NMR ($CDCl_3$, δ ppm): 7.47–6.91 (br, 12H, Ar-H), 4.29 (t, 8H, OCH_2), 3.91 (s, 8H, SCH_2), 1.95–1.24 (m, 24H, CH_2), 0.98 (t, 12H, CH_3). UV–Vis λ_{max}(nm)($\log\varepsilon$) in $CDCl_3$: 354(4.20), 687(4.55). MS (MALDI-TOF): *m*/*z* 1219.7 $[M+H]^+$Anal. Calc. for $C_{60}H_{64}N_8O_8S_4Zn$: C, 59.07; H, 5.25; N, 9.19; Found: C, 59.12; H, 5.13; N, 9.08%.

2.3. Electrochemical and spectroelectrochemical measurements

The electrochemical and spectroelectrochemical measurements were carried out with a Gamry Reference 600 potentiostat/galvanostat utilizing a three-electrode cell configuration at 25 °C. For cyclic voltammetry (CV), and square wave voltammetry (SWV) measurements, the working electrode was a Pt disc with a surface area of 0.071 cm^2. Surface of the working electrode was polished with a diamond suspension before each run. A Pt wire served as the counter electrode. Saturated calomel electrode (SCE) was employed as the reference electrode and separated from bulk of the solution by a double bridge. Ferrocene was used as an internal reference. Tetrabutylammonium perchlorate (TBAP) in dichloromethane (DCM) and dimethylsulfoxide (DMSO) was employed as the supporting electrolyte at a concentration of 0.10 mol dm^{-3}. High purity N_2 was used to remove dissolved O_2 for at least 15 min prior to each run and to maintain a nitrogen blanket during the measurements. IR compensation was applied to the CV and SWV scans to minimize the potential control error. UV/Vis absorption spectra and chromaticity diagrams were measured by an OceanOptics QE65000 diode array spectrophotometer. In-situ spectroelectrochemical measurements were carried out by utilizing a three-electrode configuration of a thin-layer quartz spectroelectrochemical cell at 25 °C. The working electrode was a Pt semi-transparent electrode. A Pt wire counter electrode separated by a glass bridge and a SCE reference electrode separated from bulk of the solution by a double bridge were used.

In-situ electrocolorimetric measurements under potentiostatic control were obtained using an OceanOptics QE65000 diode array spectrophotometer at color measurement mode by utilizing three-electrode configuration of a thin-layer quartz spectroelectrochemical cell. The standard illuminant A with 2-degree observer at constant temperature in a light booth designed to exclude external light was used. Prior to each set of measurements, background color coordinates (*x*, *y*, and *z* values) were taken at open-circuit, using the electrolyte solution without MPc under study. During the measurements, readings were taken as a function of time under kinetic control, however the color coordinates at the beginning and final of each redox processes were also reported.

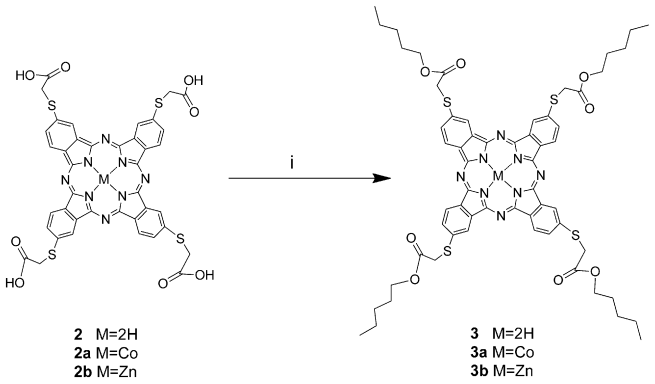

Scheme 1. Esterification of carboxy-terminated phthalocyanine derivatives, (i) DCC, p-TSA, *n*-pentanol, pyridine, 60 °C, 48 h.

3. Results and discussion

3.1. Synthesis and characterization

4-(carboxymethylsulfanyl)phthalonitrile (**1**), tetrakis(4-carboxy methylsulfanyl)-phthalocyanine (**2**), tetrakis(4-carboxymethylsul fanyl) cobalt(II) phthalocyanine (**2a**) and tetrakis(4-carboxymethyl sulfanyl) zinc(II)phthalocyanine (**2b**) were prepared as reported earlier [10]. The phthalocyanines **2**, **2a**–**b** are soluble in DMSO and DMF. The thiocarboxylic acid substituents on the phthalocyanine core bring out a vast number of possibilities for binding with different groups. To achieve a better solubility in apolar solvents, pentyl substituents were introduced into the thiocarboxy units. Esterification of all the COOH groups in **2**, **2a**–**b** with *n*-pentanol to give tetrakis(pentyloxycarbonyl methylsulfanyl)phthalocyanine **3** and metallo derivatives **3a**–**b** were accomplished in pyridine in the presence of dicyclohexylcarbodiimide and 4-toluenesulfonic acid as catalyst for 48 h at 60 °C. The byproduct dicyclohexylurea was separated from the crude products by treatment with cold ethanol for 6 h at 0 °C and then washing with cold ethanol, acetonitrile, methanol, hexane and diethyl ether several times. Products were isolated by column chromatography on silica gel first with Hexane/THF (2:1) for **3** and Hexane/THF (5:1) for **3a**–**b** then with THF as eluent with yields of 32% for **3**, 24% for **3a** and 27% for **3b**. These novel phthalocyanines show good solubility in organic solvents such as $CHCl_3$, THF, CH_2Cl_2. All compounds were identified through various spectroscopic techniques such as ^1H NMR, FT-IR, UV–vis, mass spectra, and elemental analysis. The results obtained were in agreement with the predicted structures given in Scheme 1.

In the IR spectra, the presence of C=O peaks around 1726–1729 cm^{-1} and O–C=O stretches around 1130–1137 cm^{-1}, aromatic and aliphatic stretching C–H peaks around

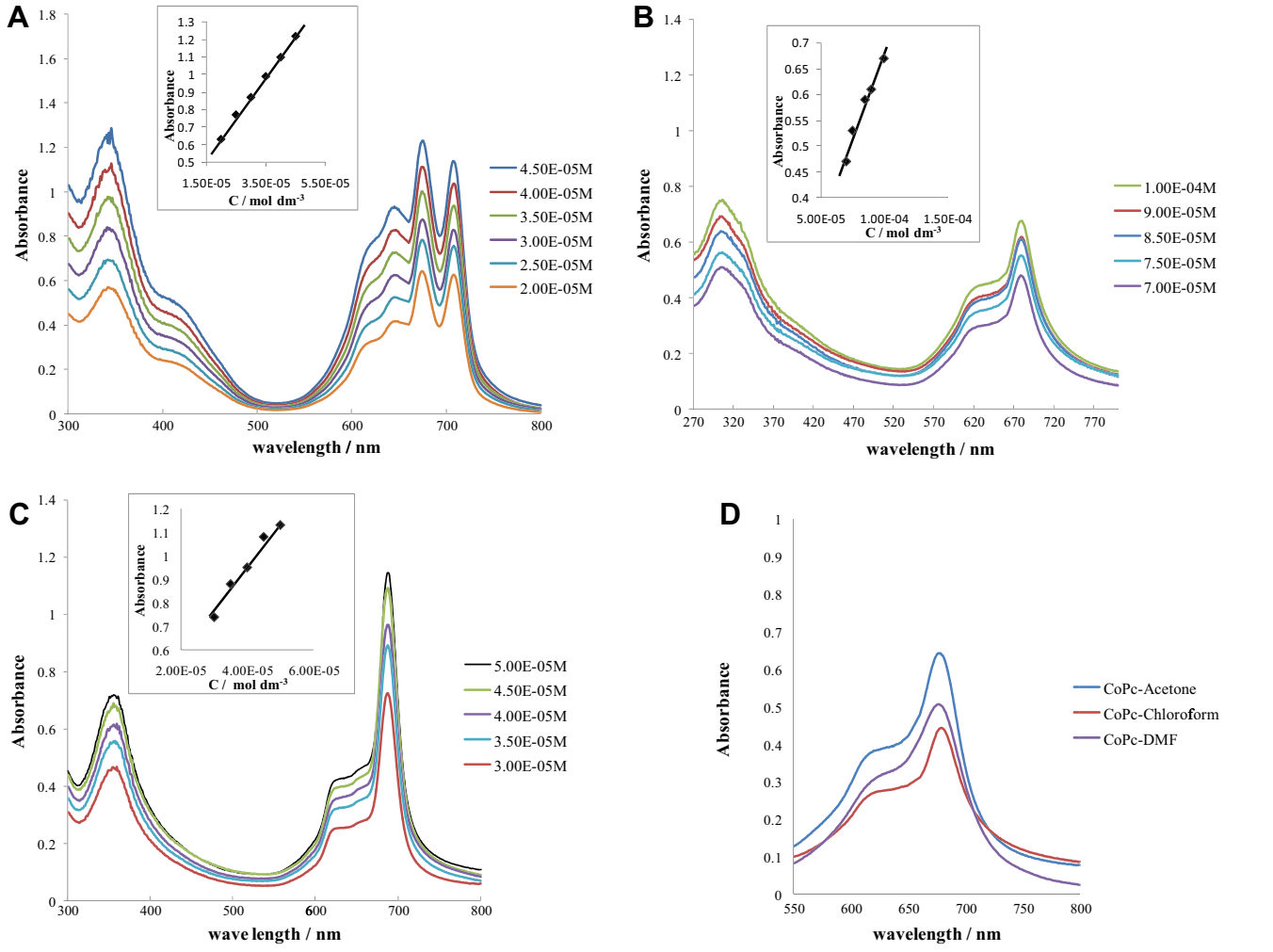

Fig. 1. Changes in the electronic spectra of **3** (a), **3a** (b), **3b** (c) with different concentrations in chloroform and Q bands of compound **3a** (D)(6×10^{-5} mol dm^{-3}) in different solvents.

Table 1
UV–Vis data for the phthalocyanines in chloroform(**3**, **3a**–**b**) and THF(**2**, **2a**–**b**).

Compound	λ, nm (log ε, M^{-1} cm^{-1})			Reference
2	348(4.39)	684(4.43)	710(4.41)	[10]
2a	325(4.25)	679(4.36)		[10]
2b	345(4.56)	684(4.53)		[10]
3	342(4.61)	675(4.63)	708(4.58)	
3a	315(4.13)	680(4.08)		
3b	354(4.20)	687(4.55)		

2850–3080 cm^{-1} and the disappearance of the intense broad carboxylic acid O–H peaks around 3600–2500 cm^{-1} together with the high solubility in chloroform acquired after this reaction, are all evidences for the formation of **3**, **3a**–**b**. The carboxylic acid C=O peaks of the phthalocyanines **2**, **2a**–**b** around 1714 cm^{-1} were shifted to higher frequencies around 1726–1729 cm^{-1} after esterification. These results were in harmony with the literature and have been a good evidence for esterification process.

Most significant differences between ^1H NMR spectra of compounds **2**, **2a**–**b** and **3**, **3a**–**b** are the disappearance of carboxylic –OH chemical shifts in the latter and appearance of new chemical shifts at around δ 4.30, 1.97–1.24 and 0.86 ppm attributable to aliphatic protons. ^1H NMR investigations of these compounds provided the characteristic chemical shifts for the expected structures.

The mass spectral (MALDI-TOF) results of pentyloxy carbonylmethylsulfanyl-substituted cobalt phthalocyanine **3a** confirmed the complete esterification of COOH groups by the presence of molecular ion peaks, at *m*/*z* 1213.6.

The phthalocyanines **3**, **3a**–**b** (Fig. 1) show typical electronic spectra with two strong absorption regions, one of them in the UV region at about 300–400 nm (B band) arising from the deeper π-levels → LUMO transition and the other in the visible part of the spectrum around 600–700 nm (Q band) attributed to the π–π* transition from the highest occupied molecular orbital (HOMO) to the lowest unoccupied molecular orbital (LUMO) of the Pc^{-2} ring (Tables 1 and 2). These two bands are typical for all phthalocyanines. The Q band splits in metal-free phthalocyanine due to a D_{2h} symmetry [1–3]. The electronic absorption spectrum of the metal-free phthalocyanine **3** exhibits a partly split Q band absorption at 708 and 675 nm and the B band of this Pc appeared in the UV region at 342 nm. The Q band absorption of metallophthalocyanines is observed as a single band of high intensity in the visible region. The metallophthalocyanines **3a**–**b** showed the expected absorptions of the Q bands at 680, 687 nm and B bands at 315, and 354 nm, respectively.

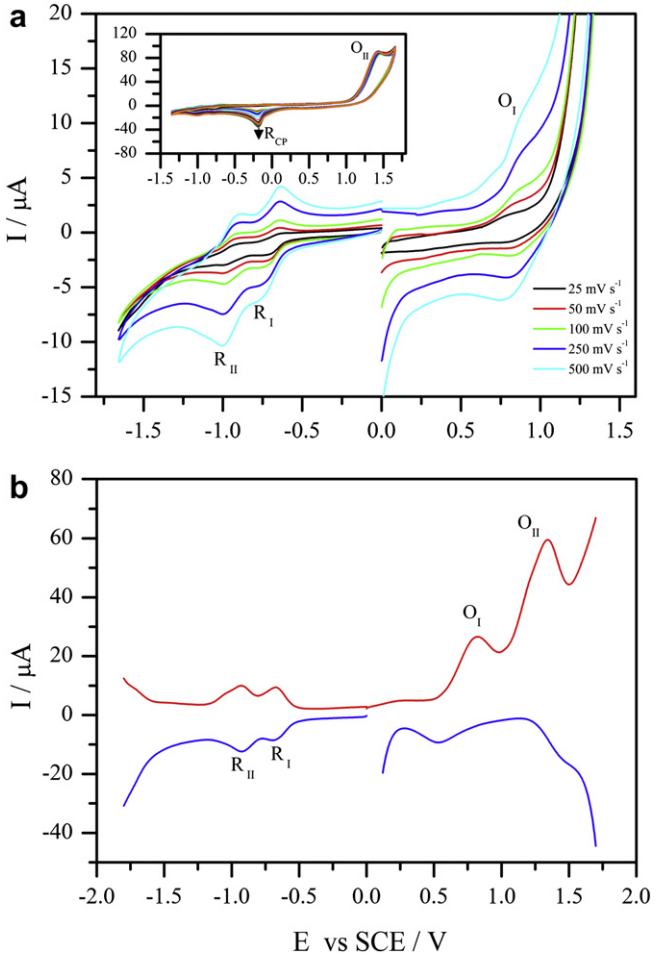

Fig. 2. a) CVs of **H_2Pc** (**3**) (5.0×10^{-4} mol dm^{-3}) various scan rates in CM/TBAP electrolyte system on Pt working electrode (Inset: repetitive CVs of **H_2Pc**). b) SWV of **H_2Pc** (**3**), SWV parameters: pulse size = 100 mV; Step Size: 5 mV; Frequency: 25 Hz.

As frequently encountered in most phthalocyanines, weaker absorptions on the higher energy side of Q bands indicate the presence of aggregated species which are generally observed together with the main Q bands essentially responsible for the

Table 2
Voltammetric data of the complexes.

Complex		Ring oxidations	M^{III}/M^{II}	M^{II}/M^{I}		Ring reductions			[d]$\Delta E_{1/2}$
H_2Pc (in DCM)	[a]$E_{1/2}$ vs. SCE	[e]1.34	0.82			−0.67	−0.91	–	1.49
	[b]ΔE_p (mV)	–	–			75	70	–	
	[c]I_{pa}/I_{pc}	–	–			0.94	0.86	–	
ZnPc (in DCM)	[a]$E_{1/2}$ vs. SCE	1.41	0.74 (0.60)			−0.98 (−0.86)	−1.18	–	1.45
	[b]ΔE_p (mV)	–	83			87	92	–	
	[c]I_{pa}/I_{pc}	–	0.94			0.97	0.55	–	
CoPc (in DCM)	[a]$E_{1/2}$ vs. SCE		0.84		−0.22 (−0.71)	−1.01			1.06
	[b]ΔE_p (mV) vs. SCE		–		123	–			
	[c]I_{pa}/I_{pc}		–		0.88	–			
CoPc (in DMSO)	[a]$E_{1/2}$ vs. SCE		0.87	0.30	−0.55 (−1.00)	−1.55			0.85
	[b]ΔE_p (mV) vs. SCE		–	80	77	65			
	[c]I_{pa}/I_{pc}		–	0.98	1.18	0.95			

[a] $E_{1/2} = (E_{pa} + E_{pc})/2$ at 0.100 V s^{-1}.
[b] $\Delta E_p = |E_{pa} - E_{pc}|$.
[c] I_{pa}/I_{pc} for reduction, I_{pc}/I_{pa} for oxidation processes at 0.100 V s^{-1} scan rate.
[d] $\Delta E_{1/2} = E_{1/2}$ (first oxidation) – $E_{1/2}$ (first reduction) = HOMO–LUMO gap for metallophthalocyanines having electro-inactive metal center.
[e] The process is recorded with SWV.

intense absorption occurring due to the monomeric species [1]. When the electronic spectra of the metal-free phthalocyanine (**3**) and its zinc and cobalt derivatives (**3a**–**b**) were carefully examined, weak peaks were observed around 620–640 nm just on the higher energy side of the strong Q band. In order to see whether these bands are a consequence of aggregation or not has been investigated by measuring absorption spectra in a concentration range [17]. In the concentration ranges studied, no aggregation tendency has been observed as it is shown by the linear change of absorbance in Q band maxima (Lambert-Beer law) for the monomeric species with respect to the concentration (Fig. 1). In addition to chloroform, more polar solvents have been tried in the case of **3b** to observe the relation between polarity of the solvent and aggregation tendency for this molecule (Fig. 1d); when the polarity increased, the peak corresponding to aggregated species did not show parallel increase which is indicative of non-aggregation of the phthalocyanine compound in solvents studied.

3.2. Electrochemical measurements

Solution redox properties of the complexes were studied using CV and SWV measurements in DCM and/or DMSO on the platinum electrode. Table 1 lists the assignments of the redox couples and the electrochemical parameters, which included half-wave peak potentials ($E_{1/2}$), anodic to cathodic peak potential separation (ΔE_p), ratio of anodic to cathodic peak currents (I_{pa}/I_{pc}), and difference between the first oxidation and reduction potentials ($\Delta E_{1/2}$). Peak to peak separations, $E_{1/2}$ and $\Delta E_{1/2}$ values are in agreement with the

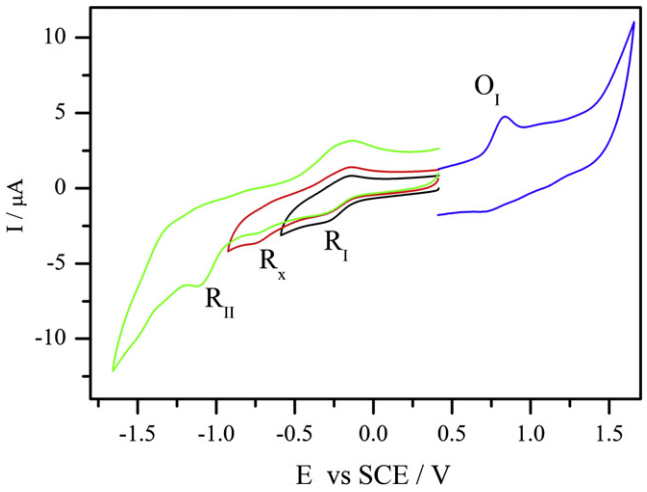

Fig. 4. CVs of **CoPc** (**3a**) (5.0×10^{-4} mol dm^{-3}) at 0.100 V s^{-1} scan rate in DCM/TBAP electrolyte system on Pt working electrode.

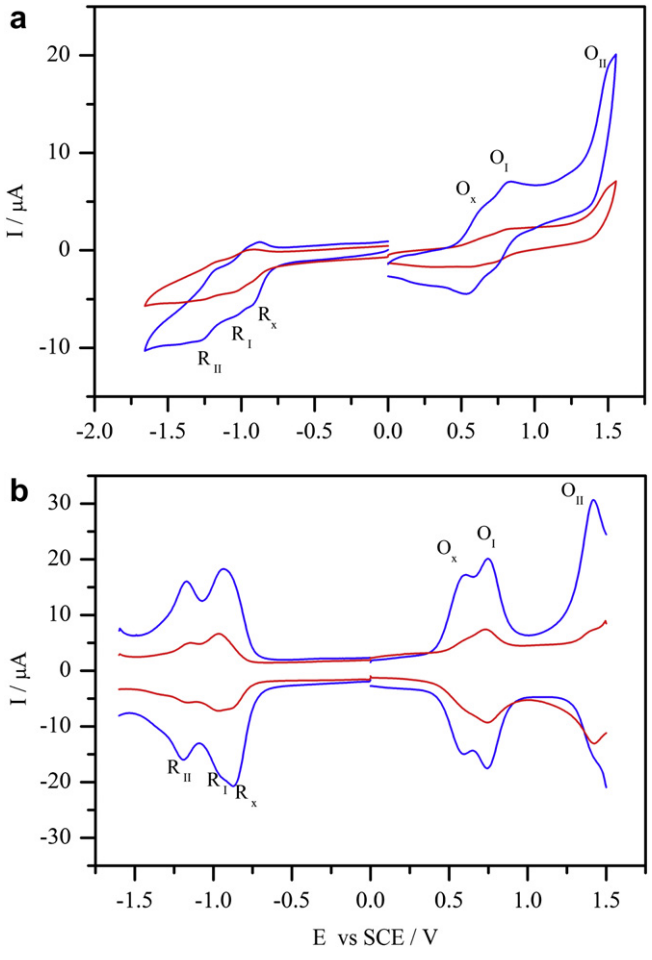

Fig. 3. a) CVs of **ZnPc** (**3b**) (blue CV: 5.0×10^{-4} mol dm^{-3}, red CV: 2.0×10^{-4} mol dm^{-3}) at 0.100 V s^{-1} scan rate in DCM/TBAP electrolyte system on Pt working electrode. b) SWV of **ZnPc** (**3b**) (blue SWV: 5.0×10^{-4} mol dm^{-3}, red SWV: 2.0×10^{-4} mol dm^{-3}), SWV parameters: pulse size = 100 mV; Step Size: 5 mV; Frequency: 25 Hz. (For the interpretation of the reference to color in this figure legend, the reader is referred to the web version of this article.)

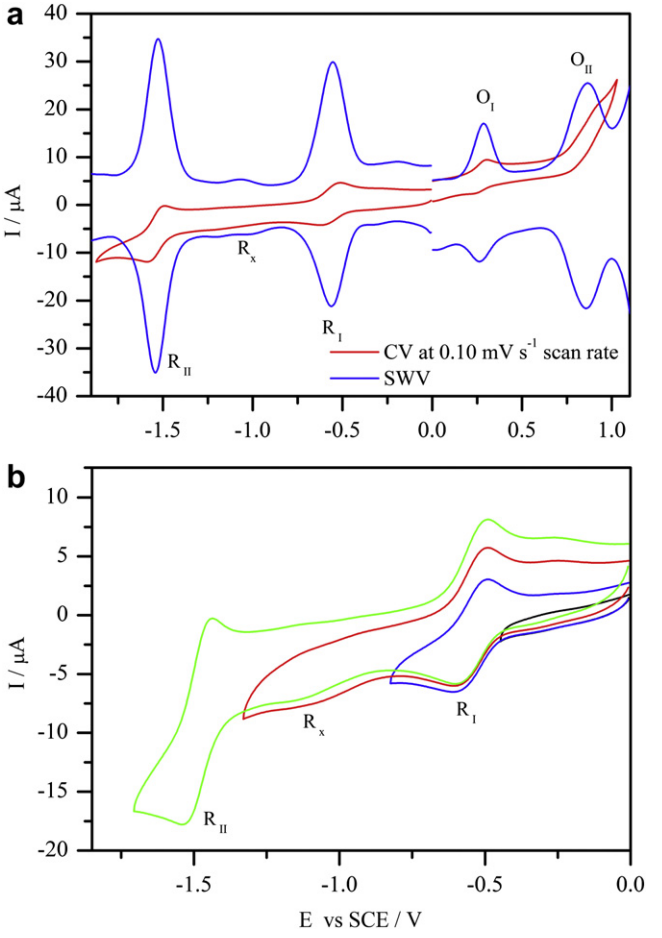

Fig. 5. a) CVs and SWVs of **CoPc** (**3a**) (5.0×10^{-4} mol dm^{-3}) at 0.100 V s^{-1} scan rate in DMSO/TBAP electrolyte system on Pt working electrode. (SWV parameters: pulse size = 100 mV; Step Size: 5 mV; Frequency: 25 Hz). b) CVs of **CoPc** (**3a**) recorded with different cathodic vertex potentials.

reported data for redox processes of the metallo-phthalocyanine complexes [7,18–21]. $\Delta E_{1/2}$ reflects the HOMO–LUMO gap for metal-free Pcs and it is related with HOMO–LUMO gap in MPc species having redox inactive metal center.

H_2Pc (**3**) and **ZnPc** (**3b**) indicate voltammetric responses with small potential shifts due to the different Pc ring centers of the complexes. Based on the well-known electrochemical behaviors of these phthalocyanine complexes, all redox couples of the complexes are assigned to the phthalocyanine ring [7,18–21]. Nature of the redox couples of **3b** will also be confirmed by using *in-situ* spectroelectrochemical measurements given below. Fig. 2 shows CV and SWV of **H_2Pc** (**3**), which indicates a one-electron oxidation and two one-electron reduction couples. For the reduction couples, ΔE_p values change from 60 to 120 mV with the increasing scan rate; suggest electrochemical reversibility of the electron transfer process [22]. Theoretically, for a system that is both electrochemically and chemically reversible, ΔE_p should be $0.059/n$ independent of scan rate. In practical applications, ΔE_p of a couple is compared with that of universal indicator ferrocene/ferrocenium couple. In our system, ΔE_p's were changed from 60 to 110 mV for ferrocene with increasing scan rates from 0.010 to 1.00 V s^{-1}. The effect of coupled chemical reactions to the electron transfer reactions is illustrated with I_{pa}/I_{pc} ratio change as a function of the scan rate and I_p changes as a function of the square root of the scan rate ($(I_{pc} - \nu^{1/2})$). While I_{pa}/I_{pc} ratios of the reduction processes are smaller than unity at slow scan rates, I_{pa}/I_{pc} ratios get unity at higher scan rates, which indicates the kinetic complication of the electrochemically reversible reduction processes. Moreover, the first oxidation process at 0.80 V has an irreversible peak character and followed with an intense second oxidation process at 1.34 V. As shown in Fig. 2a inset, **H_2Pc** (**3**) gives a new peak at −0.19 V when potential is switched after this second oxidation process. The peak current of this wave recorded at −0.19 V increases with the repetitive CV scan. These data indicate electropolymerization of the complex at more positive potential and the polymerized film gives reduction at −0.19 V.

Fig. 3 represents CV and SWV of **ZnPc** (**3b**). Within the potential window of DCM/TBAP electrolyte system, two reductions (labeled $\mathbf{R_I}$ at −0.86 V and $\mathbf{R_{II}}$ at −1.18 V) and two oxidation processes (labeled $\mathbf{O_I}$ at 0.74 V and $\mathbf{O_{II}}$ at 1.41 V) are recorded with **ZnPc** (**3b**) (Fig. 3a). The first oxidation and first reduction processes split due to the aggregation of the species. Diluting the solution decreases the peak current of the waves (R_x and O_x) assigned to the aggregated species more than that of the monomeric species supporting the existence of an aggregation–disaggregation equilibrium. SWV scans support the recorded wave and their aggregation character (Fig. 3b).

Electrochemical analysis of **CoPc** (**3a**) in TBAP/DMSO electrolyte system does not give well defined CV and SWV responses due to the aggregation of the complex in this electrolyte system (Fig. 4). Redox processes split due to the presence of different aggregated species. Spectral measurements indicate the aggregation of the complex in

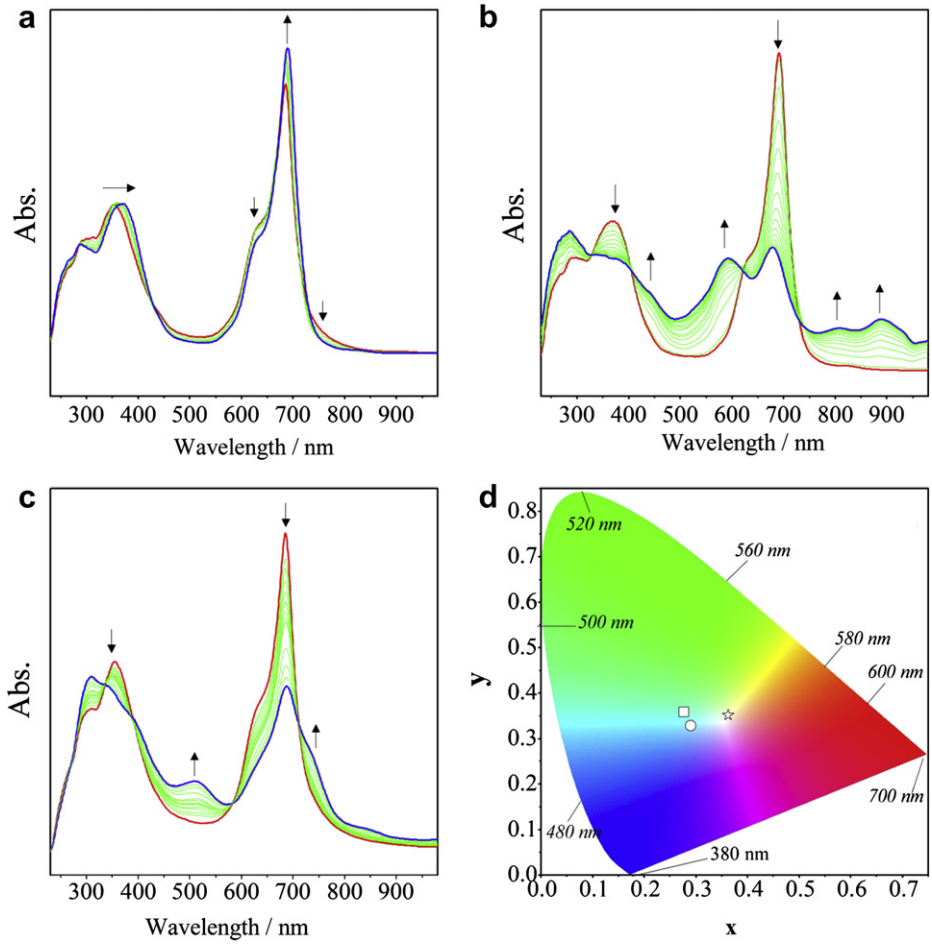

Fig. 6. *In-situ* UV–vis spectral changes of **ZnPc** (**3b**). a) initial part of the spectral changes at $E_{app} = -1.05$ V. b) final part of the spectral changes at $E_{app} = -1.05$ V. c) $E_{app} = 0.90$ V. d) Chromaticity diagram of **ZnPc** (**3b**). (Each symbol represents the color of electro-generated species; □: $[Zn^{II}Pc^{-2}]$, ○: $[Zn^{II}Pc^{-3}]^{-1}$, ☆: $[Zn^{II}Pc^{-1}]^{+1}$.

high extend. Thus electrochemical analysis of **3a** is performed in a coordinating solvent (DMSO) to prevent the aggregation of the complex. This complex gives two one-electron oxidation and two one-electron reduction couples during the CV measurements within the electrochemical window of TBAP/DMSO (Fig. 5). As shown in Fig. 5 aggregation of the complex is diminished, so a small wave assigned to the aggregated species is recorded at −1.00 V. CV responses of the complex is recorded with different vertex potentials as shown in Fig. 5b and differentiating the cathodic switching potential does not affect the VC responses of the complex. With respect to ΔE_p and I_{pa}/I_{pc} ratios, both reduction couples have reversible and diffusion controlled peak characters in DMSO/TBAP electrolyte system. Similarly oxidation couples have quasi-reversible peak characters.

3.3. Spectroelectrochemical studies

Spectroelectrochemical studies were employed to confirm the assignments in the CVs of the complexes. Fig. 6 shows the spectral chances of **ZnPc** (**3b**) as a representative of MPc's having redox inactive metal center under applied potential. During the controlled potential reductions of **3b** at −1.05 V potential application, first of all while the Q band at 685 nm increases in intensity with shifting to 690 nm the band assigned to the aggregated species at 630 nm decreases due to the shifting of the aggregation–disaggregation equilibrium under applied potential (Fig. 6a). At the same time the B band at 352 nm shifts to 372 nm. Then while the Q band decreases in intensity without shift, new bands are recorded at 588, 805, and 888 nm (Fig. 6b). Moreover the B band at 372 nm decreases in intensity during the first reduction process. During this electrochemical reduction, clear isosbestic points are observed at 330, 403, 622, and 735 nm, which demonstrate that reduction gives a single product. These spectroscopic changes indicate presence of an aggregation–disaggregation equilibrium and a Pc ring reduction process and assign the first reduction process (couple R_1) to $[Zn^{II}Pc^{-2}]/[Zn^{II}Pc^{-3}]^{-1}$ process [23–28]. Spectroscopic changes under controlled potential application at −1.30 V supported the further reduction of the monoanionic $[Zn^{II}Pc^{-3}]^{-1}$ species to $[Zn^{II}Pc^{-4}]^{-2}$. During the oxidation of **ZnPc** (**3b**) (Fig. 6c), the absorption of the Q band decreases in intensity without shift, while new bands at 511 and 740 nm appears with increasing in intensity. Clear isosbestic points were recorded at 388, 583, and 713 nm in the spectra. These changes are typical of the ring-based oxidation and assigned to $[Zn^{II}Pc^{-2}]/[Zn^{II}Pc^{-1}]^{+1}$ process [23–28].

The color change of the solution of the complexes during the redox processes was recorded using *in-situ* colorimetric measurements Without any potential application, the solution of **ZnPc** (**3b**) is bluish green ($x = 0.2776$ and $y = 0.3583$) (Fig. 6d). As the potential is stepped from 0 to −1.05 V color of the neutral $[Zn^{II}Pc^{-2}]$ start to changes and light blue color ($x = 0.2898$ and $y = 0.3287$) of monoanionic form of $[Zn^{II}Pc^{-3}]^{-1}$ was obtained at the end of the first reduction. Similarly color of the monocationic species, $[Zn^{II}Pc^{-1}]^{+1}$ has yellow color ($x = 0.3631$ and $y = 0.3511$).

Fig. 7 indicates *in-situ* UV–vis spectral changes and *in-situ* recorded chromaticity diagram of **CoPc**(**3a**). During the potential

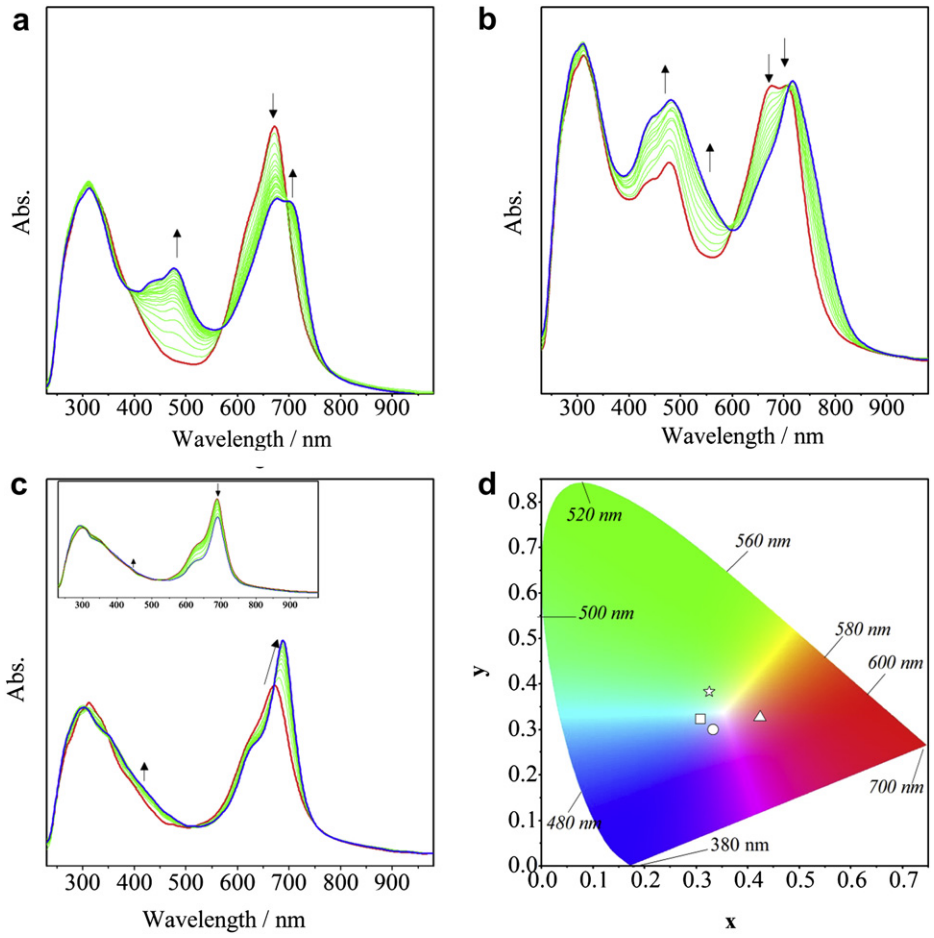

Fig. 7. *In-situ* UV–vis spectral changes of **CoPc** (**3a**). a) $E_{app} = -0.70$ V. b) $E_{app} = -1.70$ V. c) $E_{app} = 0.50$ V (Inset: $E_{app} = 1.00$ V). d) Chromaticity diagram of **CoPc** (**3a**). (Each symbol represents the color of electro-generated species; □: $[Co^{II}Pc^{-2}]$, ○: $[Co^{I}Pc^{-2}]^{-1}$, △: $[Co^{I}Pc^{-2}]^{-}$, ☆: $[Co^{III}Pc^{-1}]^{+2}$.

application at −0.70 V, the Q band at 673 nm decreases in intensity and a new band is recorded at 710 nm. At the same time a new band increases at 477 nm in intensity. Increasing a band between 400 and 500 nm and decreasing the Q band with shift characterize formation of $Co^{I}Pc^{2-}$ species (Fig. 7a). This process gives clear isosbestic points at 388, 568, and 692 nm in the spectra and a color change from blue ($x = 0.3091$ and $y = 0.3226$) to purple ($x = 0.3328$ and $y = 0.2992$). These spectroscopic data confirm our earlier assignment of the process R_1 to $[Co^{II}Pc^{-2}]/[Co^{I}Pc^{-2}]^{1-}$ process [23–28]. Further reduction of the $[Co^{I}Pc^{-2}]^{1-}$ at −1.70 V indicates the ring-based redox process. Because the Q band at 710 nm remain as unchanged, while the intensity of the region at around 500 nm increases with the band at 477 nm. During this process, presence of the band at 477 nm indicates the Co^{I} oxidation state of the central metal (Fig. 6b). Clear isosbestic points were observed at 600 and 710 nm in the spectra. Color change from purple to red ($x = 0.4242$ and $y = 0.3258$) was recorded. These changes assign the process R_{II} to $[Co^{I}Pc^{-2}]^{1-}/[Co^{I}Pc^{-3}]^{2-}$. Fig. 7c represents the spectral changes during the oxidation processes of the complex. During 0.50 V potential application, the Q band increases with red shifting to 690 nm, which indicates the $[Co^{III}Pc^{-2}]^{+1}$ formation during the first oxidation process (Fig. 7c). Then the Q band decreases without shift while a new weak band try to increase at 455 nm (Fig. 7c inset) during the second oxidation process at 1.00 V. However this band do not increase obviously, which may be due to the decomposition of the complex after the second oxidation process. Observation of a new band at 455 nm and decreasing the Q band without shift indicate the ring-based process and assigned to $[Co^{III}Pc^{-2}]^{+1}/[Co^{III}Pc^{-1}]^{+2}$ process. These *in-situ* spectral changes are in agreement with the literature, which clearly stated that metal oxidation occurs before ring oxidation in **3a** complexes in coordinating solvents [18]. Color changes from blue to green ($x = 0.326$ and $y = 0.382$) were recorded during the first oxidation process (Fig. 7d).

4. Conclusions

The synthesis, characterization, voltammetric and spectroelectrochemical properties of newly synthesized tetrakis(pentyloxycarbonylmethylsulfanyl) substituted metal-free and metallophthalocyanine derivatives have been presented in this work for the first time. Voltammetric and spectroelectrochemical studies show that while metal-free and zinc phthalocyanine complexes give ring-based, multi-electron and reversible/*quasi*-reversible redox processes, cobalt phthalocyanine complex give both metal and ring-based, diffusion controlled, multi-electron and reversible/*quasi*-reversible reduction processes. Definite determination of the colors of the electro-generated anionic and cationic form of the complexes is important to decide the possible electrochromic application of the complexes.

Acknowledgment

This work was supported by the Research Fund of the Technical University of Istanbul.

References

[1] Leznoff CC, Lever ABP. Phthalocyanines properties and applications. Weinheim: VCH Publishers; 1989.
[2] Moser FH, Thomas AL. Properties in: the phthalocyanines, vol. 1. Boca Raton, FL: CRC Press; 1983.
[3] McKeown NB. Phthalocyanine materials: synthesis, structure and function. Cambridge: Cambridge University Press; 1998.
[4] Kobayashi N, Ogata H, Nonaka N, Luk'yanets EA. Effect of peripheral substitution on the electronic absorption and fluorescence spectra of metal-free and zinc phthalocyanines. Chem Eur J 2003;9(20):5123–34.
[5] Dabak S, Gümüş G, Gül A, Bekaroğlu Ö. Synthesis and properties of new phthalocyanines with tertiary or quaternarized aminoethylsulfanyl substituents. J Coord Chem 1996;38(4):287–93.
[6] Sevim AM, Hojiyev R, Gül A, Çelik MS. An investigation of the kinetics and thermodynamics of the adsorption of a cationic cobalt porphyrazine onto sepiolite. Dyes Pigments 2011;88(1):25–38.
[7] Osmanbaş ÖA, Koca A, Özceşmeci İ, Okur Aİ, Gül A. Voltammetric, spectroelectrochemical, and electrocatalytic properties of thiol-derivatized phthalocyanines. Electrochim Acta 2008;53(15):4969–80.
[8] Arslanoğlu Y, Sevim AM, Hamuryudan E, Gül A. Near-IR absorbing phthalocyanines. Dyes Pigments 2006;68(2–3):129–32.
[9] Uslu Kobak RZ, Öztürk ES, Koca A, Gül A. The synthesis and cyclotetramerisation reactions of aryloxy-, arylalkyloxy-substituted pyrazine-2,3-dicarbonitriles and spectroelectrochemical properties of octakis(hexyloxy)-pyrazinoporphyrazine. Dyes Pigments 2010;86(2):115–22.
[10] Sevim AM, Ilgün C, Gül A. Preparation of heterogeneous phthalocyanine catalysts by cotton fabric dyeing. Dyes Pigments 2011;89(2):162–8.
[11] Atsay A, Koca A, Kocak MB. Synthesis, electrochemistry and in situ spectroelectrochemistry of water-soluble phthalocyanines. Trans Met Chem 2009;34(8):877–90.
[12] Sağlam Ö, Gül A. Porphyrazines with appending eight crown ethers. Polyhedron 2001;20:269–75.
[13] Dinçer HA, Gonca E, Gül A. The synthesis and spectral properties of novel phthalocyanines with pendant bulky units. Dyes Pigments 2008;79(2):166–9.
[14] Yenilmez HY, Okur Aİ, Gül A. Peripherally tetra-palladated phthalocyanines. J Organomet Chem 2007;692(5):940–5.
[15] Akkurt B, Hamuryudan E. Enhancement of solubility via esterification: synthesis and characterization of octakis (ester)-substituted phthalocyanines. Dyes Pigments 2008;79(2):153–8.
[16] Young JG, Onyebuagu W. Synthesis and characterization of di-disubstituted phthalocyanines. J Org Chem 1990;55(7):2155–9.
[17] Çamur M, Özkaya AR, Bulut M. Novel phthalocyanines bearing four 4-phenyloxyacetic acid functionalities. Polyhedron 2007;26(12):2638–46.
[18] Lever ABP, Milaeva ER, Speier G. The redox chemistry of metallophthalocyanines in solution. In: Leznoff CC, Lever ABP, editors. Phthalocyanines: properties and applications, vol. 3. New York: VCH; 1993. p. 5–27.
[19] Günsel A, Kandaz M, Koca A, Salih B. Functional fluoro substituted tetrakis-metallophthalocyanines: synthesis, spectroscopy, electrochemistry and spectroelectrochemistry. J Fluor Chem 2008;129(8):662–8.
[20] Özer M, Altındal A, Özkaya AR, Bulut M, Bekaroğlu Ö. Synthesis, characterization and some properties of novel bis(pentafluorophenyl)methoxyl substituted metal free and metallophthalocyanines. Polyhedron 2006;25:3593–602.
[21] Koca A, Özkaya AR, Selçukoğlu M, Hamuryudan E. Electrochemical and spectroelectrochemical characterization of the phthalocyanines with pentafluorobenzyloxy substituents. Electrochim Acta 2007;52(7):2683–90.
[22] Kissinger PT, Heineman WR. Laboratory techniques in electroanalytical chemistry. 2nd ed. New York: Marcel Dekker; 1996. pp. 51–163.
[23] Simicglavaski B, Zecevic S, Yeager E. Spectroelectrochemical in situ studies of phthalocyanines. J Electrochem Soc 1987;134(3):C130.
[24] Agboola B, Ozoemena KI, Nyokong T. Synthesis and electrochemical characterisation of benzylmercapto and dodecylmercapto tetra substituted cobalt, iron, and zinc phthalocyanines complexes. Electrochim Acta 2006;51:4379–87.
[25] Kulaç D, Bulut M, Altındal A, Özkaya AR, Salih B, Bekaroğlu Ö. Synthesis and characterization of novel 4-nitro-2-(octyloxy)phenoxy substituted symmetrical and unsymmetrical Zn(II), Co(II) and Lu(III) phthalocyanines. Polyhedron 2007;26(18):5432–40.
[26] Koca A, Bayar Ş, Dinçer HA, Gonca E. Voltammetric, in-situ spectroelectrochemical and in-situ electrocolorimetric characterization of phthalocyanines. Electrochim Acta 2009;54(10):2684–92.
[27] Nombona N, Nyokong T. The synthesis, cyclic voltammetry and spectroelectrochemical studies of Co(II) phthalocyanines tetra-substituted at the α and β positions with phenylthio groups. Dyes Pigments 2009;80(1):130–5.
[28] Mbambisa G, Tau P, Antunes E, Nyokong T. Synthesis and electrochemical properties of purple manganese(III) and red titanium(IV) phthalocyanine complexes octa-substituted at non-peripheral positions with pentylthio groups. Polyhedron 2007;26(18):5355–64.